

## DEPTH CONVERSION OF ZERO-OFFSET AND TIME-MIGRATED REFLECTIONS

*M. Tygel, B. Ursin, E. Iversen, and M.V. de Hoop*

**email:** *mtygel@gmail.com*

**keywords:** *CRS, time migration, reflector dip, reflector curvature, anisotropy*

### ABSTRACT

*The surface-to-surface propagator matrix of a given (central) reflection ray, which connects a measurement surface to a target reflector, permits us to express the parabolic or hyperbolic traveltimes of paraxial rays in an appealing and useful way. In the case the central ray is a normal (or image) ray, the initial and end dislocations of any paraxial normal (or image) ray are coupled. This leads to an interesting consequence time-to depth conversion of zero-offset (stacked) or time-migrated reflections. Under a given depth velocity background model if the traveltimes and its first and second derivatives are known for a given reflection, we present a unified approach to map that reflection into its reflector depth location and also to estimate the reflector dip and curvature. The obtained explicit expressions for the reflector dip and curvature can be useful constraints in the process of time-to-depth conversion or map migration of stacked or time-migrated data*

### INTRODUCTION

Time-to-depth conversion of selected events, either from stacked (simulated zero-offset (ZO)) or time-migrated (TM) sections, are very useful tools to obtain first depth images of target reflectors. Obtained in generally fast and efficient way, such images help to construct or validate complex velocity models for later imaging procedures (e.g., pre-stack depth migration), in which the computational effort is much significant. In our previous paper, Tygel et al. (2009), we addressed the problem of providing a meaning to the first and second derivatives of an identified time-migrated reflections. We have shown that these quantities, which are nothing else than the Common-Reflection-Surface (CRS) stack method applied to time-migration data, relate to the dip and curvature of the target reflector at the points where the image rays from the surface hit that reflector. Under the knowledge of a macro-velocity in depth, an explicit formula was provided for the reflector dip in terms of the first derivative (slope) of the time-migrated reflection traveltimes and quantities depending on the central image ray only. A second explicit formula was given for the curvature of the target reflector in terms of the second derivative of the time-migrated reflection traveltimes and quantities depending on image rays in the vicinity of the central image ray. Here, that previous paper will be extended in following accounts:

- (a) A new formula for the curvature of the target reflector is provided, in which the (unpleasant) dependency on neighboring (paraxial) rays to the central image ray has been eliminated. Numerical tests confirm the accuracy of the formula;
- (b) The theory described for time-migrated data has been extended to ZO (stacked) data. In other words, explicit relationships between first and second derivatives of ZO traveltimes and reflector dip and curvature have been derived;

## FORMULATION

In the following we shall consider as seismic data a *stacked volume* or a *time-migrated volume*. Coordinates for the data points within these volumes are  $(\mathbf{m}, T)$ , where  $\mathbf{m}$  designates trace location (for example, a CMP location), and  $T$  is (stacked or time-migrated) time.

In both stacked or time-migrated volumes, we consider a reflection event for a target (unknown) reflector. For traces,  $\mathbf{m}$ , in the vicinity of the reference trace,  $\mathbf{m} = \mathbf{0}$ , the parabolic Taylor approximation of traveltime has, in both volumes, the form

$$T(\mathbf{m}) = T_0 + \mathbf{m}^T \boldsymbol{\lambda} + \frac{1}{2} \mathbf{m}^T \boldsymbol{\Lambda} \mathbf{m}, \quad (1)$$

where  $T_0 = T(\mathbf{0})$  is the traveltime along the central ray and

$$\boldsymbol{\lambda} = \frac{\partial T}{\partial \mathbf{m}} \quad \text{and} \quad \boldsymbol{\Lambda} = \frac{\partial^2 T}{\partial \mathbf{m} \partial \mathbf{m}^T}, \quad (2)$$

all derivatives being evaluated at  $\mathbf{m} = \mathbf{0}$ . Under the assumption that the quantities  $T_0$ ,  $\boldsymbol{\lambda}$  and  $\boldsymbol{\Lambda}$  have been estimated from the data, and also assuming that a background velocity model is available, it is our aim to invert the dip and curvature of the target reflector at the point the central ray hits the reflector. To simplify the analysis, we assume that the measurement surface is planar horizontal and that the same 2D Cartesian coordinates,  $\mathbf{m}$ , simultaneously locate the ZO (stacked) trace and the initial point of the normal ray that corresponds to that trace. In the same way, the time-migrated trace and the initial point of the image ray that correspond to that point. In particular,  $\mathbf{m} = \mathbf{0}$  locates the reference ZO (resp. time-migrated) trace and reference normal (image) ray. The following two situations are envisaged here:

- (a) **ZO (stacked) data:** For a stacked volume, taken as a simulated zero-offset (ZO) volume, equation 1 represents the response of the target reflector under ZO illumination. As a consequence,  $T(\mathbf{m})$  defines twice the traveltime of the normal ray, issued at the location,  $\mathbf{m}$ , at the measurement surface, to the target reflector. As well known, the linear vector coefficient,  $\boldsymbol{\lambda}$ , represents the tangential projection of the slowness vector (or ray-parameter vector) of the downgoing normal ray at its initial (central) point. Under the use of the given depth-velocity model, that normal ray can be traced into depth until it reaches the (unknown) target reflector when half the given ZO traveltime, namely  $T_0/2$ , is consumed.
- (b) **Time-migrated data:** For a time-migrated volume, equation 1 represents the response of the target reflector under the illumination of image rays. As a consequence,  $T(\mathbf{m})$ , defines twice the traveltime of the image ray, issued at the location  $\mathbf{m}$  at the measurement surface to the target reflector. By definition, the slowness vector of the initial point of the image ray is normal to the measurement surface. Setting the initial point to be the central point, and under the use of the given depth-velocity model, the central image ray can be traced into depth until it reaches the (unknown) target reflector, which occurs when half the given image-ray traveltime, namely  $T_0/2$ , is consumed.

From the above considerations, a first reconstruction of the target reflector can be obtained by the endpoints of central rays, once their traveltime and slowness vectors at their initial points have been estimated. Of course, such construction will be much more accurate if, not only the traveltime, but also the reflector dip and curvature can be also estimated at the reflector points. As seen below, these are quantities that will be derived from the coefficients  $\boldsymbol{\lambda}$  and  $\boldsymbol{\Lambda}$  estimated from the data.

From now on, we focus our attention on a single central (normal or image) ray, attached to the central point,  $\mathbf{m} = \mathbf{0}$ , and assume that the quantities  $T_0$ ,  $\boldsymbol{\lambda}$  and  $\boldsymbol{\Lambda}$  have been already estimated. Based on the previous discussion, we also assume that the central ray, which starts at central point and has its endpoint at the reflector, has been traced and its dynamical quantities computed. It is our aim to determine, from these quantities, the dip and curvature of the target reflector.

**Coordinate systems:** Attached to our selected central ray, it is important to introduce the appropriate coordinate systems, so as to formulate and solve our problem in a most simple and effective way. To facilitate the exposition, we consider that the measurement surface,  $\mathcal{M}$ , planar and that points on that

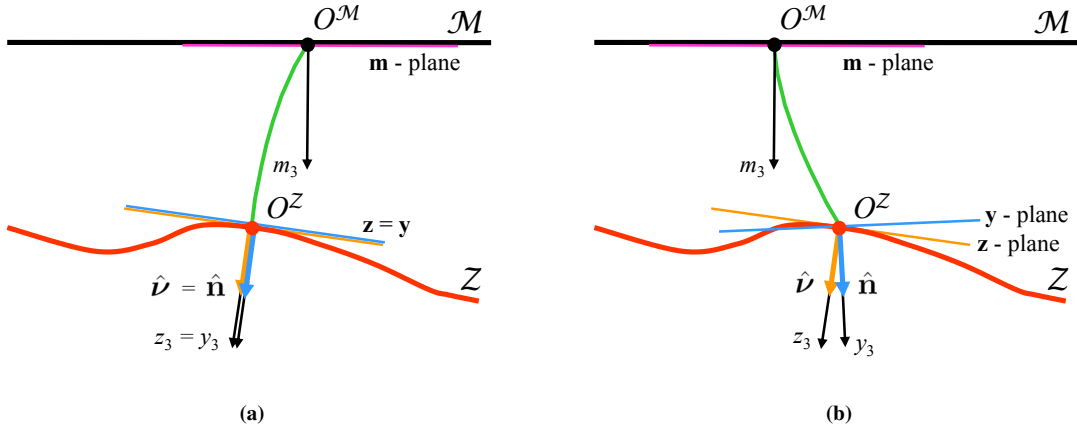


**Figure 1:** Coordinate systems: (a) Central ray is the normal ray; (b) Central ray is the image ray.

surface in the vicinity of the initial point of the central ray can be located by the same coordinates,  $\mathbf{m}$ , that specify the stacked or time-migrated traces. Concerning the target reflector, denoted by  $\mathcal{Z}$ , we consider the following two coordinate systems:

- (a) The *wavefront coordinate system*: Denoted by the  $\hat{\mathbf{y}}$ -system, this 3D Cartesian coordinate system has its origin at the end (reflector) point,  $O^Z$ , of the ray and is such that its  $y_3$ -axis points in the direction of the slowness vector of the ray at that point. Such direction is known by the ray-tracing procedure and denoted as  $\hat{\mathbf{n}}$ . In symbols, we have

$$\hat{\mathbf{y}}_3 = \hat{\mathbf{n}}, \quad (3)$$

where  $\hat{\mathbf{y}}_3$  is the unitary vector in the  $y_3$  direction. Located at the plane normal to  $\hat{\mathbf{n}}$ , the remaining axes,  $y_1$  and  $y_2$ , can be arbitrarily chosen, so that a positively oriented Cartesian system is obtained. Quantities (e.g., coordinates, vectors, matrices) referred to the  $\hat{\mathbf{y}}$ -system will be marked with a superscript,  $Y$ . In the  $\hat{\mathbf{y}}$ -coordinates, the slowness and ray-velocity vectors are written

$$\hat{\mathbf{p}}^Y = \begin{pmatrix} \mathbf{0} \\ 1/c \end{pmatrix}, \quad \hat{\mathbf{v}}^Y = \begin{pmatrix} \mathbf{v}^Y \\ c \end{pmatrix}. \quad (4)$$

The vector  $\mathbf{v}^Y$  is zero if the medium is isotropic at the actual ray/interface intersection point.

- (b) The *reflector coordinate system*: Denoted by the  $\hat{\mathbf{z}}$ -system, this 3D Cartesian system also has its origin at the end (reflector) point,  $O^Z$ , of the ray. It is such that, now, its  $z_3$ -axis points in the direction of the normal to the reflector at  $O^Z$ . Such direction is known for the normal ray but *not known* for the image ray, being denoted by  $\hat{\mathbf{v}}$ . In symbols, we have

$$\hat{\mathbf{z}}_3 = \hat{\mathbf{v}}, \quad (5)$$

where  $\hat{\mathbf{z}}_3$  is the unitary vector in the  $z_3$  direction. Located at the plane normal to  $\hat{\mathbf{v}}$ , the remaining axes,  $y_1$  and  $y_2$ , can be arbitrarily chosen, so that a positively oriented Cartesian system is obtained. Quantities referred to the  $\hat{\mathbf{z}}$ -system will be marked with a superscript,  $Z$ . In the vicinity of the point  $O$ , and using  $\hat{\mathbf{z}}$  coordinates, the reflector is assumed in the form

$$z_3 = \Sigma^Z(\mathbf{z}), \quad (6)$$

with the properties

$$\Sigma^Z(\mathbf{0}) = 0, \quad \frac{\partial \Sigma^Z}{\partial \mathbf{z}}(\mathbf{0}) = \mathbf{0}, \quad \text{and} \quad \frac{\partial^2 \Sigma^Z}{\partial \mathbf{z} \partial \mathbf{z}^T}(\mathbf{0}) = -\mathbf{D}, \quad (7)$$

where  $\mathbf{D}$  is the reflector curvature matrix. The two left-most equations above incorporate the fact that the reflector is tangent to the  $\mathbf{z}$ -axis at the origin,  $O^Z$ . In view of the above considerations, any point on the reflector, sufficiently close to  $O$ , is completely determined by a 2D-coordinate vector,  $\mathbf{z}$ , together with a third coordinate,  $z_3$ , satisfying equation 7. We see that the determination of the reflector dip and curvature is equivalent to the determination of the vector,  $\hat{\mathbf{v}}$ , and matrix,  $\mathbf{D}$ , respectively.

A detailed description of the general properties, and in particular the transformation between the two systems is provided in Appendix A.

### TRAVELTIMES OF PARAXIAL RAYS

In the framework of the propagator matrix theory described in Appendix B, the (one-way) traveltimes of a paraxial image ray that joins the point  $\mathbf{m}$  at  $\Sigma^M$  to the point  $\mathbf{z}$  at  $\Sigma^Z$  can be expressed as

$$t(\mathbf{m}, \mathbf{z}) = t_0 - \mathbf{m}^T \mathbf{p}^M + \mathbf{z}^T \mathbf{p}^Z - \mathbf{m}^T \mathbf{B}^{-1} \mathbf{z} + \frac{1}{2} \mathbf{m}^T \mathbf{B}^{-1} \mathbf{A} \mathbf{m} + \frac{1}{2} \mathbf{z}^T \mathbf{D} \mathbf{B}^{-1} \mathbf{z}. \quad (8)$$

Here, the quantities  $\mathbf{A}$ ,  $\mathbf{B}$ ,  $\mathbf{C}$  and  $\mathbf{D}$  are the  $2 \times 2$  component submatrices of the propagator matrix of the central, one-way, (normal or image) ray (see Appendix B. Moreover,

$$t_0 = T_0/2 \quad (9)$$

is the traveltimes along the central ray. The linear coefficients

$$\mathbf{p}^M = \frac{\partial t}{\partial \mathbf{m}} \quad \text{and} \quad \mathbf{p}^Z = \frac{\partial t}{\partial \mathbf{z}}, \quad (10)$$

are the projection of the slowness vector of the central ray on the tangent plane to the measurement and reflector surfaces at its initial and endpoints, respectively. Finally, the quadratic coefficients are given by

$$\frac{\partial^2 t}{\partial \mathbf{m} \partial \mathbf{m}^T} = \mathbf{B}^{-1} \mathbf{A}, \quad \frac{\partial^2 t}{\partial \mathbf{z} \partial \mathbf{z}^T} = \mathbf{D} \mathbf{B}^{-1} \quad \text{and} \quad \frac{\partial^2 t}{\partial \mathbf{m} \partial \mathbf{z}^T} = -\mathbf{B}^{-1}. \quad (11)$$

All derivatives in equations 10 and 11 are evaluated at  $\mathbf{m} = \mathbf{z} = \mathbf{0}$ . Slowness projection vectors are known as *apparent slowness* or *ray parameters*. As a consequence, the slowness vectors,  $\hat{\mathbf{p}}^M$  of the downgoing central ray at its initial (central) point is given by

$$\hat{\mathbf{p}}^M = (\mathbf{p}^M, p_3^M), \quad \text{with} \quad p_3^M = \sqrt{(1/c^M)^2 - \mathbf{p}^{M^T} \mathbf{p}^M}, \quad (12)$$

where  $c^M$  is the phase velocity of the medium at that central point. An analogous expression holds, of course, for  $\hat{\mathbf{p}}^Z$ .

### Traveltimes of paraxial rays with coupled initial and endpoints

As seen below, for stacked or time-migrated reflections, the initial and endpoints of the corresponding paraxial rays are connected or, more specifically, there is a functional dependence  $\mathbf{z} = \mathbf{z}(\mathbf{m})$ . For our purposes, it suffices to use a second-order Taylor approximation of  $\mathbf{z}(\mathbf{m})$ , namely

$$z_I = u_{IJ} x_J + h_{KL}^I x_K x_L, \quad (13)$$

where  $u_{IJ}$  and  $h_{KL}^I$  are the components of the matrices

$$\mathbf{U} = \left( \frac{\partial z_I}{\partial x_J} \right) \quad \text{and} \quad \mathbf{H}^I = \left( \frac{\partial^2 z_I}{\partial x_K \partial x_L} \right). \quad (14)$$

Substituting equation 13 into equation 8, we obtain the traveltimes as a function of the single variable  $\mathbf{m}$ . Retaining terms up to second order only, that traveltimes can be written, in vector form, as

$$\mathcal{T}(\mathbf{m}) = t(\mathbf{m}, \mathbf{z}(\mathbf{m})) = \mathcal{T}_0 + \mathbf{m}^T \mathbf{p} + \frac{1}{2} \mathbf{m}^T \mathbf{M} \mathbf{m}, \quad (15)$$

where

$$\mathbf{p} = \mathbf{U}^T \mathbf{p}^Z - \mathbf{p}^M \quad \text{and} \quad \mathbf{M} = \mathbf{V} + \boldsymbol{\varepsilon}, \quad (16)$$

with

$$\mathbf{V} = (\mathbf{U}^T \mathcal{D} - 2\mathbf{I}) \mathcal{B}^{-1} \mathbf{U} + \mathcal{B}^{-1} \mathcal{A}, \quad (17)$$

and

$$\boldsymbol{\varepsilon} = (\varepsilon_{IJ}), \quad \text{with} \quad \varepsilon_{IJ} = p_K^Z h_{IJ}^K. \quad (18)$$

Comparison of the resulting traveltime with the input traveltime 1 provides the relationships between the input quantities,  $T_0$ ,  $\boldsymbol{\lambda}$  and  $\boldsymbol{\Lambda}$ , and the corresponding output quantities which contain the sought-for reflector dip and curvature. More specifically, we have

$$\mathcal{T} = \frac{1}{2} T_0, \quad \mathbf{p} = \frac{1}{2} \boldsymbol{\lambda} \quad \text{and} \quad \mathbf{M} = \frac{1}{2} \boldsymbol{\Lambda}, \quad (19)$$

with  $\mathbf{p}$  and  $\mathbf{M}$  being given by equations 16-18.

### ZO (STACKED) REFLECTIONS

For a stacked reflection, the central and paraxial rays are both normal rays. Then the condition  $\mathbf{p}^Z = \Delta \mathbf{p}^Z = \mathbf{0}$  holds. Substitution into equation B-2 and solving the system for  $\mathbf{z}$  and  $\mathbf{m}$ , yields, to first order in  $\mathbf{m}$ , the relation

$$\mathbf{z} = \mathbf{U} \mathbf{m} = \mathcal{D}^{-T} \mathbf{m}, \quad (20)$$

where equation B-4 has been used. Substitution of equation 20 into equation 17 yields

$$\mathbf{V} = \mathcal{B}^{-1} (\mathcal{A} - \mathcal{D}^{-T}) = \mathcal{D}^{-1} \mathcal{C}, \quad (21)$$

where the right-most equation was obtained under the use of equations B-3 and B-4. Moreover, the fact that  $\mathbf{p}^Z = \mathbf{0}$  also implies that

$$\mathbf{p} = -\mathbf{p}^M, \quad \boldsymbol{\varepsilon} = \mathbf{0} \quad \text{and} \quad \mathbf{M} = \mathbf{V} = \mathcal{D}^{-1} \mathcal{C}. \quad (22)$$

Comparison between equations 1 and 15 provides the conditions

$$\mathbf{p}^M = -\frac{1}{2} \boldsymbol{\lambda}, \quad \text{and} \quad \mathcal{D}^{-1} \mathcal{C} = \frac{1}{2} \boldsymbol{\Lambda}. \quad (23)$$

The above equation tells us that, as the quantities,  $T_0$ ,  $\boldsymbol{\lambda}$  and  $\boldsymbol{\Lambda}$  are assumed to be already estimated from the data, the corresponding quantities  $\mathbf{p}^M$  and  $\mathbf{M}^M$  are also estimated. As explained earlier and still under the assumption of a given velocity model, this means that that the point where the central ray hits the reflector can be determined. In the present situation that the central ray is a normal ray, that endpoint is referred to as the *normal-incidence-point (NIP)*.

#### Reflector dip: Stacked (ZO) situation

For a normal ray, the slowness vector and normal vector at its (reflector) endpoint coincides, namely,

$$\hat{\boldsymbol{\nu}} = \hat{\mathbf{n}}. \quad (24)$$

The above equation determines the reflector dip. Moreover, following the recipe of equation A-7, we have that the coordinate systems  $\hat{\mathbf{z}}$  and  $\hat{\mathbf{y}}$  also coincide, meaning that the transformation matrix between the two systems is the  $3 \times 3$  identity matrix,  $\hat{\mathbf{G}} = \hat{\mathbf{I}}$  and also  $\mathbf{G} = \mathbf{I}$ . From equations B-5 and B-7, the matrices  $\mathcal{A}$  and  $\mathcal{B}$  are readily find to be

$$\mathcal{A} = (\mathbf{I} - \mathbf{A}^{an})^{-T} \mathbf{Q}_E \quad \text{and} \quad \mathcal{B} = (\mathbf{I} - \mathbf{A}^{an})^{-T} \mathbf{Q}_E, \quad (25)$$

respectively.

### Reflector curvature: Stacked (ZO) situation

In view of the above considerations, it turns out that the curvature matrix,  $\mathbf{D}$ , is the only unknown in the submatrix components,  $\mathcal{C}$  and  $\mathcal{D}$  of the propagator matrix. The reflector curvature can be derived upon the use of the rightmost equation 23, together with equations B-6 and B-8. To do that, we first recast equation 23 as

$$\frac{1}{2}\Lambda\mathcal{D} = \mathcal{C} \quad (26)$$

and also rewrite equations B-6 and B-8 as

$$\begin{aligned} \mathcal{C}\mathcal{A}^{-1} &= -p_3^Z\mathbf{D} + \mathcal{C}_0\mathcal{A}^{-1}, \\ \mathcal{D}\mathcal{B}^{-1} &= -p_3^Z\mathbf{D} + \mathcal{D}_0\mathcal{B}^{-1}, \end{aligned} \quad (27)$$

where we have introduced the auxiliary matrices, which are all known from the given velocity model.

$$\mathcal{C}_0\mathcal{A}^{-1} = \mathbf{E} - \mathcal{A}^{-T}\mathbf{Q}_E\mathbf{P}_E\mathcal{A}^{-1} \quad \text{and} \quad \mathcal{D}_0\mathcal{B}^{-1} = \mathbf{E} - \mathcal{B}^{-T}\mathbf{Q}_D\mathbf{P}_D\mathcal{B}^{-1}. \quad (28)$$

We finally rewrite equation 26 as

$$\frac{1}{2}(\mathcal{D}\mathcal{B}^{-1})\mathcal{B}\Lambda = (\mathcal{C}\mathcal{A}^{-1})\mathcal{A}, \quad (29)$$

and substitute equations C-5. After some algebra, this yields

$$\mathbf{D} = \frac{1}{p_3^Z} \left( \mathcal{C}_0 - \frac{1}{2}\mathcal{D}_0\Lambda \right) \left( \mathcal{A} - \frac{1}{2}\mathcal{B}\Lambda \right)^{-1}. \quad (30)$$

### TIME-MIGRATED REFLECTIONS

For a time-migrated reflection, the central and paraxial rays are both image rays. As a consequence, the condition  $\mathbf{p}^M = \Delta\mathbf{p}^M = \mathbf{0}$  holds. Substitution into equation B-2 and solving the system for  $\mathbf{z}$  and  $\mathbf{m}$ , yields, to first order in  $\mathbf{m}$ , the relation

$$\mathbf{z} = \mathbf{U}\mathbf{m} = \mathcal{A}\mathbf{m}. \quad (31)$$

Substitution of  $\mathbf{U} = \mathcal{A}$  into equations 16-17 yields

$$\mathbf{p} = \mathcal{A}^T\mathbf{p}^Z \quad \text{and} \quad \mathbf{V} = (\mathcal{A}^T\mathcal{D} - \mathbf{I})\mathcal{B}^{-1}\mathcal{A} = \mathcal{C}^T\mathcal{A}, \quad (32)$$

where the right-most equation was obtained under the use of equations B-3 and B-4. Comparison between equations 1 and 15 provides the conditions

$$\mathcal{A}^T\mathbf{p}^Z = \frac{1}{2}\boldsymbol{\lambda}, \quad \text{and} \quad \mathbf{M} = \mathcal{C}^T\mathcal{A} + \boldsymbol{\varepsilon} = \frac{1}{2}\Lambda. \quad (33)$$

In this situation, the  $\mathbf{p}^Z$  and  $\mathbf{M}$  are now the quantities that are estimated by the data inputs  $T_0$ ,  $\boldsymbol{\lambda}$  and  $\Lambda$ . As explained earlier and still under the assumption of a given velocity the point where the central ray hits the reflector can be determined by tracing downwards the image ray (defined by the condition  $\mathbf{p}^M = \mathbf{0}$ ) until the traveltimes,  $\mathcal{T} = T_0/2$  has been consumed. That point is referred to as the *image incident point (IIP)*.

We are now ready to compute the reflector dip and curvature for a ZO (stacked) or time migrated reflection if the time-domain quantities  $T_0$ ,  $\boldsymbol{\lambda}$  and  $\Lambda$  have been estimated from the data. We observe, in passing, that the image-ray field corresponds to an exploding reflector initial condition at the measurement surface in the time-migration domain. We can therefore take  $\mathbf{Q}_E$  as the  $2 \times 2$  geometric spreading matrix belonging to the image-ray wavefront.

### Reflector dip: TM situation

Following equation A-6, to obtain the reflector dip it suffices to determine the vector  $\mathbf{f}$ . In view of left-most equations A-5 and 33, we can readily write

$$\mathbf{f} = \frac{1}{2} \mathbf{G}^{-1} \mathcal{A}^{-T} \boldsymbol{\lambda}. \quad (34)$$

Moreover, from equations A-5, 35 and B-5, we have

$$\mathbf{G}^{-1} \mathcal{A}^{-T} = \mathbf{G}^{-1} [(\mathbf{G} - \mathbf{A}^{an}) \mathbf{Q}_E^{-T}] = \mathbf{G}^{-1} [(\mathbf{G} - \mathbf{G} \mathbf{f} \mathbf{v}^{YT}) \mathbf{Q}_E^{-T}] = (\mathbf{I} - \mathbf{f} \mathbf{v}^{YT}) \mathbf{Q}_E^{-Y}. \quad (35)$$

Substitution into equation 34 yields,

$$\mathbf{f} = \frac{c}{2} (1 + \kappa)^{-1} \mathbf{Q}_E^{-T} \boldsymbol{\lambda}, \quad \text{with} \quad \kappa = \frac{1}{2} \mathbf{v}^{YT} \mathbf{Q}_E^{-T} \boldsymbol{\lambda}, \quad (36)$$

which applies to anisotropic conditions at the point where the image ray hits the reflector. For isotropic conditions,  $\kappa = 0$  and equation 36 reduces to the simple result

$$\mathbf{f} = \frac{c}{2} \mathbf{Q}_E^{-T} \boldsymbol{\lambda}. \quad (37)$$

### Reflector curvature: TM situation

In the following we use equations C-23 and C-24 from Appendix A which connects the curvature matrix to second derivatives of surface-to-surface traveltime. Together with equation 33, we obtain

$$\frac{1}{2} \boldsymbol{\Lambda} = \mathbf{C}_0^T \mathcal{A} - \frac{1}{v_3^Z} \mathcal{A}^T \mathbf{D} \mathcal{A}, \quad (38)$$

where,  $\mathbf{C}_0$  is given by the leftmost equation 28. Minor rearrangement of equation 38 yields

$$\mathbf{D} = v_3^Z \left( \mathbf{C}_0 \mathcal{A}^{-1} - \frac{1}{2} \mathcal{A}^{-T} \boldsymbol{\Lambda} \mathcal{A}^{-1} \right). \quad (39)$$

### Computation of matrix $\boldsymbol{\mathcal{E}}$

We recall that matrix,  $\boldsymbol{\mathcal{E}}$ , has been introduced in the general traveltime formulas 15- 16 to account for the second-order dependence of  $\mathbf{z}$  with respect to  $\mathbf{m}$ . In the present case of TM reflections, we have from equations 33, 38 and 27,

$$\begin{aligned} \boldsymbol{\mathcal{E}} &= \frac{1}{2} \boldsymbol{\Lambda} - \mathbf{C}^T \mathcal{A} = \left( \mathbf{C}_0^T - \mathbf{C}^T \right) \mathcal{A} - \frac{1}{v_3^Z} \mathcal{A}^T \mathbf{D} \mathcal{A}, \\ &= \left( p_3^Z - \frac{1}{v_3^Z} \right) \mathcal{A}^T \mathbf{D} \mathcal{A}. \end{aligned} \quad (40)$$

In view of the well-known relationship,  $\hat{\mathbf{v}} \cdot \hat{\mathbf{p}} = 1$ , between the group velocity,  $\hat{\mathbf{v}}$ , and the slowness vector,  $\hat{\mathbf{p}}$ , we can write, in  $z$ -coordinates

$$v_K^Z p_K^Z + v_3^Z p_3^Z = 1. \quad (41)$$

It follows that the matrix  $\boldsymbol{\mathcal{E}}$  admits the alternative expression

$$\boldsymbol{\mathcal{E}} = \left( \frac{p_3^Z v_3^Z - 1}{v_3^Z} \right) \mathcal{A}^T \mathbf{D} \mathcal{A} = -\frac{v_K^Z p_K^Z}{v_3^Z} \mathcal{A}^T \mathbf{D} \mathcal{A}. \quad (42)$$

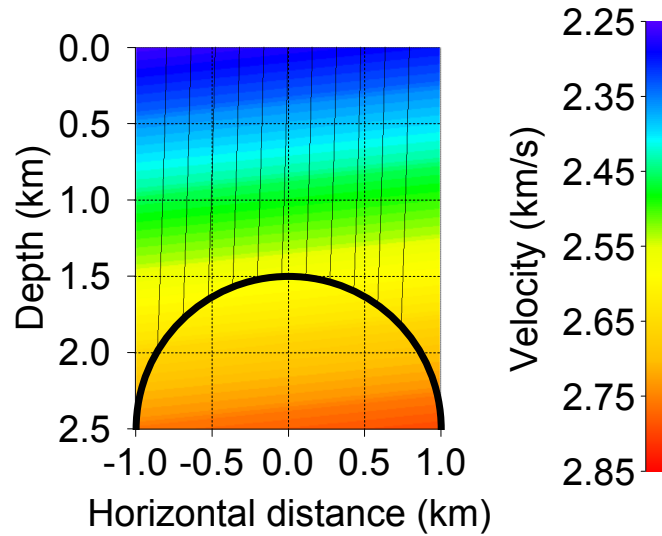


**Figure 2:** Cylindrical reflector situated in an inhomogeneous tilted transversely isotropic medium. Image ray trajectories used for generation of "observed" two-way times in the migrated domain are superimposed.

### NUMERICAL EXAMPLE

In this section we present a numerical example of mapping traveltimes belonging to the migrated time domain to corresponding parameters in the depth domain, using a known macro-velocity depth model. Observe that depth-domain coordinates are from now on referred to as  $(x, y, z)$ .

Our experiment consists of a cylindrical reflector situated in a smooth 2-D anisotropic medium as depicted in Figure 2. The anisotropy is of type TTI (tilted transversely isotropic) with a fixed symmetry axis in the direction specified by the vector  $(u_x, u_y, u_z) = (0.1, 0, 1)$  [unit]. The P-wave velocity along this axis is given by the linear function  $V_P(x, z) = 2.28 + 0.02x + 0.2z$  [km/s], while the corresponding S-wave velocities are computed using Poisson's ratio so that  $V_S(x, z) = V_P(x, z)/\sqrt{3}$ . Thomsen's parameters  $\epsilon$  and  $\delta$  have the values 0.2 and 0.1, respectively. The cylindrical reflector has its axis in the  $y$ -direction and a radius of 1 km. The axis passes through the reference point  $(0, 0, 2.5)$  [km].

To obtain synthetic measurements we traced image rays from the measurement surface until they hit the cylinder. One can observe (Figure 2) that the resulting ray trajectories are not perpendicular to the measurement surface. Computed ray traveltimes were multiplied by two and used for generation of a cubic B-spline function. From this function we obtained "measured" input parameters (times, slopes, and second derivatives) to be used for estimation of reflector depths, dips, and curvatures. Figure 3 compares analytic values of reflector depth, dip, and curvature to corresponding estimated values obtained using the true velocity model in the time-to-depth mapping procedure. The theoretical results are confirmed through this example, but it is important to remark that the curvature estimation is particularly exposed to small numerical errors as well as to measurement errors. Therefore, to obtain reliable results in "real" situations it will be critical to perform appropriate smoothing of the input time parameters. We also did a time-to-depth mapping test where anisotropy was ignored in the velocity model (Figure 4). One can then observe a significant mispositioning of the estimated reflector and corresponding systematic errors in estimated dip and curvature.

We finally show in Figure 5 that the second-order term  $\mathcal{E}$  in the curvature expression is really needed for accurate results. The reflector is still the cylinder of 1 km depicted in Figure 2, but the velocity is now homogeneous and isotropic,  $V_P = 2.5$  km/s. The departure from the constant curvature value  $1 \text{ km}^{-1}$ , gets significantly larger for increasing incident angles of the central image ray.

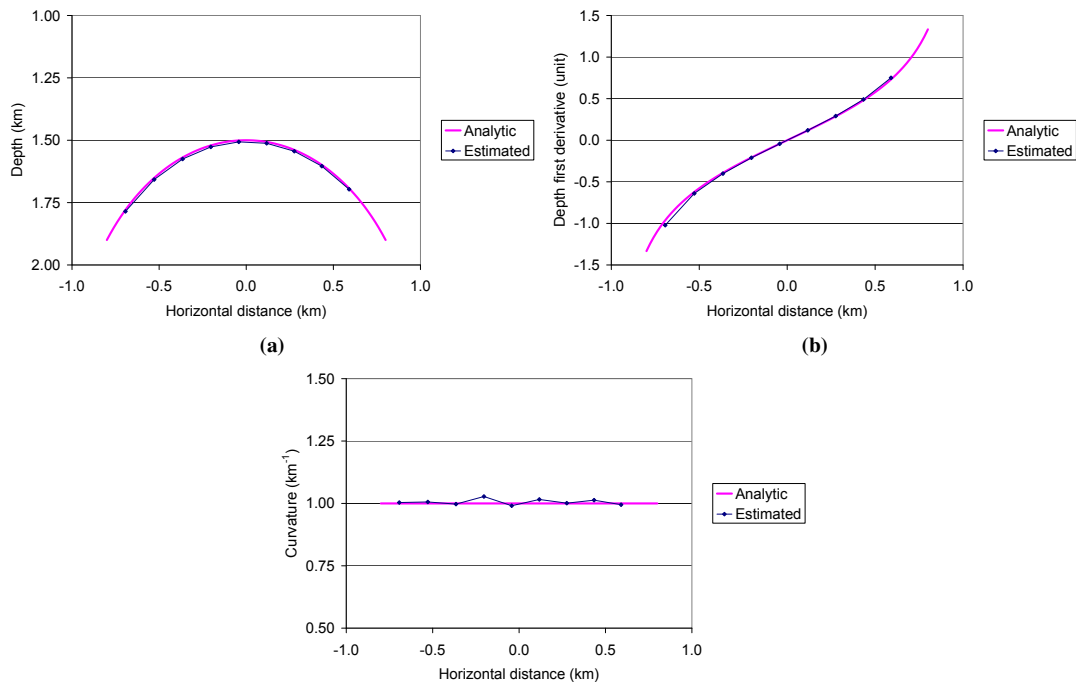


**Figure 3:** Analytic and estimated values of (a) depths, (b) dips, and (c) curvatures for the cylindrical reflector shown in Figure 2. The true anisotropic velocity model was used for image-ray time-to-depth mapping.

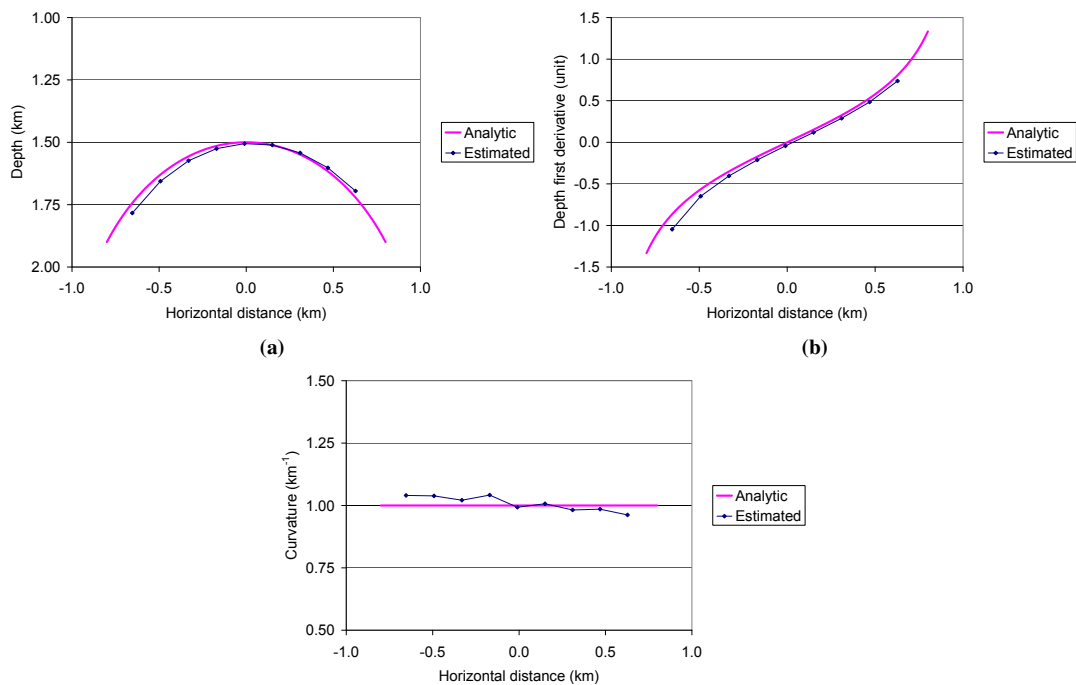


**Figure 4:** Analytic and estimated values of (a) depths, (b) dips, and (c) curvatures for the cylindrical reflector shown in Figure 2. Anisotropy was ignored in the image-ray time-to-depth mapping.

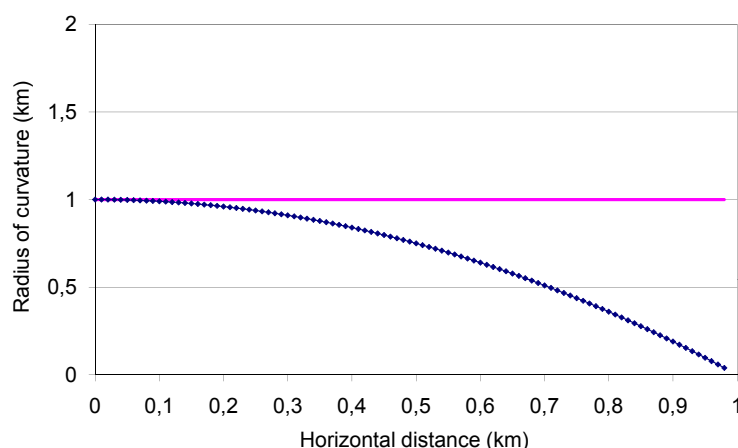


**Figure 5:** Computation of the curvature without considering the second-order term  $\mathcal{E}$ : Note how the computed curvatures (blue line) departures from the correct value (magenta line of constant radius of curvature of 1 km) for increasing horizontal distance with respect to the center of the cylinder for the initial point of the central image ray. This means the error gets larger for increasing incidence angles of the image ray.

## CONCLUSIONS

Application of the CRS method in the ZO (stacked) or time-migrated domain provides, besides a refined image, also linear and quadratic CRS coefficients. With the help of the CRS coefficients for a given ZO (stacked) or time-migrated reflection, and also under a known anisotropic background velocity model, that reflection can be mapped into the corresponding reflector. The mapping is such that, not only the location, but also the dip and curvature of the reflector are determined. This study extends previous results for CRS coefficients for time-migrated data. The obtained results are expected to be of use in mapping reflections into depth along normal or image rays.

## ACKNOWLEDGMENTS

We acknowledge support of the present work by VISTA, the *Research Council of Norway* via the ROSE project and NORSAR's SIP project 194064/I30, the *National Council of Scientific and Technological Development (CNPq)*, Brazil and the sponsors of the *Wave Inversion Technology (WIT) Consortium*, Germany.

## REFERENCES

- Červený, V. (2001). *Seismic Ray Theory*, page 461. Cambridge University Press.
- Iversen, E. (2005). Tangent vectors of isochron rays and velocity rays expressed in global Cartesian coordinates. *Studia Geophysica et Geodaetica*, 49:525–540.
- Iversen, E. (2006). Amplitude, Fresnel zone, and NMO velocity for PP and SS normal-incidence reflections. *Geophysics*, 71(02):W1–W14.
- Moser, T. J. and Červený (2007). Paraxial ray methods for anisotropic inhomogeneous media. *Geophysical Prospecting*, 55:21–37.
- Tygel, M., Ursin, B., Iversen, E., and de Hoop, M. (2009). An interpretation of crs attributes of time-migrated reflections. In *WIT Report no. 13*, pages 270–278. Wave Inversion Technology (WIT) Consortium.

### APPENDIX A: TRANSFORMATION OF WAVEFRONT AND REFLECTOR COORDINATES

We describe here the coordinate transformation between the  $\hat{\mathbf{y}}$ - and  $\hat{\mathbf{z}}$ -systems. Such transformation, which will play an important role in the derivations to follow, is simply given as a linear relationship

$$\hat{\mathbf{z}} = \hat{\mathbf{G}}\hat{\mathbf{y}}, \quad (\text{A-1})$$

where  $\hat{\mathbf{G}}$  is a  $3 \times 3$  orthonormal matrix. As such, it satisfies the relations

$$\hat{\mathbf{G}}^T \hat{\mathbf{G}} = \hat{\mathbf{G}} \hat{\mathbf{G}}^T = \hat{\mathbf{I}}. \quad (\text{A-2})$$

From basic Linear Algebra, has the form

$$\hat{\mathbf{G}} = (\hat{\mathbf{y}}_1^Z \quad \hat{\mathbf{y}}_2^Z \quad \hat{\mathbf{y}}_3^Z) = (\hat{\mathbf{z}}_1^Y \quad \hat{\mathbf{z}}_2^Y \quad \hat{\mathbf{z}}_3^Y)^T, \quad (\text{A-3})$$

where  $\hat{\mathbf{y}}_i^Z$  represents the  $i$ -th unit vector of the  $\hat{\mathbf{y}}$ -system expressed in  $\hat{\mathbf{z}}$ -coordinates. The meaning of  $\hat{\mathbf{z}}_i^Y$  is, of course, analogous. Recalling that  $\hat{\mathbf{y}}_3 = \hat{\mathbf{n}}$  and  $\hat{\mathbf{z}}_3 = \hat{\boldsymbol{\nu}}$ , we can also express the transformation matrix,  $\hat{\mathbf{G}}$ , in the alternative form (Iversen, 2005)

$$\hat{\mathbf{G}} = \begin{pmatrix} \mathbf{G} & \mathbf{n}^Z \\ \boldsymbol{\nu}^{YT} & G_{33} \end{pmatrix}, \quad \text{with } G_{33} = \hat{\boldsymbol{\nu}} \cdot \hat{\mathbf{n}} = \nu_3^Y = n_3^Z. \quad (\text{A-4})$$

Using equations A-2 and A-4 we find the useful relation

$$\mathbf{p}^Z = \mathbf{G}\mathbf{f}, \quad \text{with } \mathbf{p}^Z = \frac{1}{c}\mathbf{n}^Z \quad \text{and} \quad \mathbf{f} = -\frac{1}{\nu_3^Y}\boldsymbol{\nu}^Y. \quad (\text{A-5})$$

Here,  $\mathbf{p}^Z$  denotes the tangential component of the slowness vector of the central ray at its endpoint,  $O$ , on the reflector. The vector  $\mathbf{f}$  determines the normal unit vector to the reflector, also at point  $O$ . In wavefront coordinates, that full normal,  $\hat{\boldsymbol{\nu}}^Y$ , which defines the reflector dip, is given by

$$\hat{\boldsymbol{\nu}}^Y = \pm \frac{1}{\sqrt{1 + \mathbf{f}^T \mathbf{f}}} \begin{pmatrix} -\mathbf{f} \\ 1 \end{pmatrix}, \quad (\text{A-6})$$

where a convention for the vector direction must be specified. Besides the knowledge of the vectors,  $\hat{\mathbf{y}}_3 = \hat{\mathbf{n}}$  and  $\hat{\mathbf{z}}_3 = \hat{\boldsymbol{\nu}}$ , matrix  $\hat{\mathbf{G}}$  depends on the (non-unique) choices of the axes,  $\hat{\mathbf{y}}_I$  and  $\hat{\mathbf{z}}_I$ , which are unique up to rotation around  $\hat{\mathbf{y}}_3$  or  $\hat{\mathbf{z}}$ . Having selected the  $\hat{\mathbf{y}}$ -system, a simple choice for the axes of the  $\hat{\mathbf{z}}$ -system is

$$\hat{\mathbf{z}}_3 = \hat{\boldsymbol{\nu}}, \quad \hat{\mathbf{z}}_1 = \frac{\hat{\mathbf{y}}_2 \times \hat{\boldsymbol{\nu}}}{|\hat{\mathbf{y}}_2 \times \hat{\boldsymbol{\nu}}|} \quad \text{and} \quad \hat{\mathbf{z}}_2 = \hat{\boldsymbol{\nu}} \times \hat{\mathbf{z}}_1. \quad (\text{A-7})$$

The above definitions yield

$$\hat{\mathbf{G}} = (\hat{\mathbf{z}}_1^Y \quad \hat{\mathbf{z}}_2^Y \quad \hat{\mathbf{z}}_3^Y)^T = \begin{pmatrix} \frac{\nu_3^Y}{\nu_1^Y} & 0 & -\frac{\nu_1^Y}{\nu_3^Y} \\ -\frac{\nu_1^a \nu_2^Y}{\nu_1^Y} & a & -\frac{\nu_2^Y \nu_3^a}{\nu_3^Y} \\ \frac{\nu_1^a}{\nu_1^Y} & \nu_2^Y & \nu_3^a \end{pmatrix}, \quad \text{with } a = \sqrt{\nu_1^{Y2} + \nu_3^{Y2}}. \quad (\text{A-8})$$

Note, in particular, that if  $\hat{\mathbf{z}}_3 = \hat{\boldsymbol{\nu}}$  is parallel to  $\hat{\mathbf{y}}_3 = \hat{\mathbf{n}}$ , the transformation matrix reduces to the identity matrix,  $\hat{\mathbf{G}} = \hat{\mathbf{I}}$ .

### APPENDIX B: PROPAGATOR MATRIX OF THE CENTRAL RAY

We introduce here the theoretical useful framework of ray-propagator matrices (Červený, 2001; Moser and Červený, 2007). The basic quantity is the  $4 \times 4$  surface-to-surface propagator matrix of the downgoing, central (normal or image) ray

$$\mathcal{T} = \begin{pmatrix} \mathcal{A} & \mathcal{B} \\ \mathcal{C} & \mathcal{D} \end{pmatrix}, \quad (\text{B-1})$$

which connects the central point,  $O^M$ , on the measurement surface,  $\Sigma^M$ , to the point  $O$  on the target reflector surface,  $\Sigma^Z$ . We recall that the measurement surface, in the vicinity of the central point, is planar, with points on that surface being specified by the trace coordinates,  $\mathbf{m}$ .

**Basic properties of the propagator matrix:** For a paraxial ray, for which the variations in position and slowness are given by  $(\mathbf{m}, \Delta \mathbf{p}^M)$  (measurement surface) and  $(\mathbf{z}, \Delta \mathbf{p}^Z)$  (reflector surface), we have the relationship

$$\begin{pmatrix} \mathbf{z} \\ \Delta \mathbf{p}^Z \end{pmatrix} = \begin{pmatrix} \mathcal{A} & \mathcal{B} \\ \mathcal{C} & \mathcal{D} \end{pmatrix} \begin{pmatrix} \mathbf{m} \\ \Delta \mathbf{p}^M \end{pmatrix}. \quad (\text{B-2})$$

Moreover, we have the symplectic properties

$$\mathcal{A}\mathcal{B}^T = \mathcal{B}\mathcal{A}^T, \quad \mathcal{B}^T\mathcal{D} = \mathcal{D}^T\mathcal{B} \quad \text{and} \quad \mathcal{A}\mathcal{C}^T = \mathcal{C}\mathcal{A}^T, \quad (\text{B-3})$$

and also

$$\mathcal{A}\mathcal{D}^T - \mathcal{B}\mathcal{C}^T = \mathbf{I} \quad \text{and} \quad \mathcal{D}^T\mathcal{A} - \mathcal{C}^T\mathcal{B} = \mathbf{I}. \quad (\text{B-4})$$

**Expression of propagator matrix components:** With the help of the wavefront and reflector coordinate systems, the matrix components of the propagator matrix,  $\mathcal{T}$ , can be written as citecerveny2001,

$$\mathcal{A} = (\mathbf{G} - \mathbf{A}^{an})^{-T} \mathbf{Q}_E, \quad (\text{B-5})$$

$$\mathcal{C} = (\mathbf{E} - p_3^Z \mathbf{D}) \mathcal{A} + \mathcal{A}^{-T} \mathbf{Q}_E^T \mathbf{P}_E, \quad (\text{B-6})$$

$$\mathcal{B} = (\mathbf{G} - \mathbf{A}^{an})^{-T} \mathbf{Q}_D, \quad (\text{B-7})$$

$$\mathcal{D} = (\mathbf{E} - p_3^Z \mathbf{D}) \mathcal{B} + \mathcal{B}^{-T} \mathbf{Q}_D^T \mathbf{P}_D. \quad (\text{B-8})$$

Here, the  $2 \times 2$  matrix pairs  $(\mathbf{Q}_E, \mathbf{P}_E)$  and  $(\mathbf{Q}_D, \mathbf{P}_D)$ , correspond to hypothetical wavefront solutions initialized, respectively, as an exploding reflector (E) and a point diffractor (D) at the measurement surface (Iversen, 2006). We remark that the above-defined matrix pairs, represent an inherent property of the given central image ray and measurement surface, defined independently of the interface. The  $2 \times 2$  matrix  $\mathbf{E}$  is given by

$$E_{IJ} = \frac{1}{c} \left[ G_{I3} G_{JM} \eta_M^Y + G_{J3} G_{IK} \eta_K^Y + G_{I3} G_{J3} (\eta_3^Y - \frac{1}{c} \eta_L^Y v_L^Y) \right], \quad (\text{B-9})$$

and

$$\mathbf{A}^{an} \equiv \mathbf{p}^Z \mathbf{v}^{YT}, \quad (\text{B-10})$$

is the  $2 \times 2$  *anisotropy matrix*. Both matrices  $\mathbf{E}$  and  $\mathbf{A}^{an}$ , assumed to be already computed using the given velocity model, are introduced and described in great detail by Červený (2001). The entities  $v_i^Y$  and  $\eta_i^Y$ ,  $i = 1, 2, 3$ , are components of the ray-velocity vector  $\hat{\mathbf{v}}^Y$  and the slowness-derivative vector  $\hat{\boldsymbol{\eta}}^Y = d\hat{\mathbf{p}}^Y/dT$ , specified in wavefront coordinates. For isotropic media, we have  $\mathbf{A}^{an} = \mathbf{0}$ . It is to be observed that in many situations, one can also consider that  $\mathbf{E} = \mathbf{0}$ . For example, this is the case if the medium is locally homogeneous. Matrix  $\mathbf{E}$  is also zero if the slowness vector is normal to the interface.

In summary, we can draw the following conclusions;

- (A) The reflector dip, namely the reflector normal,  $\hat{\mathbf{v}}$ , is determined by the matrix  $\mathbf{G}$ , or equivalently, by the matrices  $\mathcal{A}$  and  $\mathcal{B}$ ;
- (B) With the knowledge of the dip, the reflector curvature,  $\mathbf{D}$ , is determined by the matrices  $\mathcal{C}$  or  $\mathcal{D}$ .

### APPENDIX C: SURFACE-TO-SURFACE TRAVELTIME RELATIONS FOR THE IMAGE-RAY FIELD

In this appendix we derive general transformations relations pertaining to an exploding-surface ray field, i.e., a ray field where individual rays are started simultaneously at a given initial (measurement) surface. The slowness vectors of the rays are normal to this surface. The rays are captured on a final (reflector) surface. The image-ray field is a special case of such exploding-surface ray fields.

We denote the standard ray coordinates for the image-ray field as  $\hat{\gamma} = (\mathbf{m}, t)$ . Here,  $t$  is the travelttime from the exploding measurement surface,  $\mathcal{M}$ . On the surface  $\mathcal{M}$  itself we therefore have  $t = 0$ . In the following, we let the measurement surface be planar and the coordinates  $\mathbf{m}$  be Cartesian such that  $\mathbf{m} = \mathbf{0}$  for a certain central ray. However, this does not imply loss of generality, as the derived relations

are valid also when  $\mathbf{m} = (m_1, m_2)$  is defined as orthogonal curvilinear coordinates for a generally shaped measurement surface. Moreover, in the following we take advantage of an alternative ray coordinate system for the exploding-surface ray field, described by the vector  $\hat{\boldsymbol{\mu}} = (\mathbf{m}, t^{\mathcal{Z}})$ . Here the parameter  $t^{\mathcal{Z}}$  is the travelttime measured from the reflector surface  $\mathcal{Z}$ . Along the surface  $\mathcal{Z}$  we have  $t^{\mathcal{Z}} = 0$ .

The travelttime parameters  $t$  and  $t^{\mathcal{Z}}$  are independent variables. However, for a point on a given ray, specified by the vector  $\mathbf{m}$ , we can connect the two parameters via the relation

$$t^{\mathcal{Z}} = t - \mathcal{T}, \quad (\text{C-1})$$

where  $\mathcal{T}$  denotes the surface-to-surface travelttime.

### General properties

Let  $S$  be an arbitrary differentiable variable which can be either a function of the ray coordinates  $\hat{\boldsymbol{\mu}}$  or the local Cartesian reflector coordinates  $\mathbf{z}$ . The chain rule for derivatives then yields

$$\frac{\partial S}{\partial \mu_i} = \frac{\partial S}{\partial z_m} \frac{\partial z_m}{\partial \mu_i}. \quad (\text{C-2})$$

In particular, if  $S = \mu_k$ , one obtains the well-known relation between the forward transformation matrix  $(\partial z_m / \partial \mu_i)$  and its inverse  $(\partial \mu_k / \partial z_m)$ ,

$$\frac{\partial \mu_k}{\partial z_m} \frac{\partial z_m}{\partial \mu_i} = \delta_{ki}. \quad (\text{C-3})$$

We make the following observations:

- The partial derivatives  $\partial z_M / \partial m_I$  are taken for constant  $t^{\mathcal{Z}}$ . When  $t^{\mathcal{Z}} = 0$  we can identify these derivatives as the elements of  $2 \times 2$  submatrix  $\mathcal{A}$  of the  $4 \times 4$  surface-to-surface propagator matrix, i.e.,

$$\mathcal{A}_{MI} = \frac{\partial z_M}{\partial m_I}. \quad (\text{C-4})$$

- The first partial derivatives of  $z_3$  with respect to  $m_I$  are also taken for constant  $t^{\mathcal{Z}}$ . When  $\mathbf{m} = \mathbf{0}$  and  $t^{\mathcal{Z}} = 0$  we have

$$\frac{\partial z_3}{\partial m_I} = 0. \quad (\text{C-5})$$

To derive the above result, we observe that, if  $t^{\mathcal{Z}} = 0$ , points are on the reflector, namely  $z_3 = \Sigma^{\mathcal{Z}}(\mathbf{z})$ . As a consequence, keeping  $t^{\mathcal{Z}} = 0$ , we have

$$\frac{\partial z_3}{\partial m_I} = \frac{\partial \Sigma^{\mathcal{Z}}}{\partial z_M} \frac{\partial z_M}{\partial m_I}. \quad (\text{C-6})$$

Equation C-5 now follows, since  $\mathbf{z} = \mathbf{0}$  when  $\mathbf{m} = \mathbf{0}$  and  $t^{\mathcal{Z}} = 0$  and also  $(\partial \Sigma^{\mathcal{Z}} / \partial z_M)(\mathbf{0}) = 0$ , we have  $\mathbf{z} = \mathbf{0}$ ,

- Partial differentiation with respect to  $t$  and  $t^{\mathcal{Z}}$  is equivalent, since  $\mathbf{m}$  is kept constant in both situations. Therefore, we have

$$\frac{\partial z_M}{\partial t^{\mathcal{Z}}} = \frac{\partial z_M}{\partial t} = v_M^{\mathcal{Z}}, \quad \frac{\partial z_3}{\partial t^{\mathcal{Z}}} = \frac{\partial z_3}{\partial t} = v_3^{\mathcal{Z}}. \quad (\text{C-7})$$

- Considering only differentiation with respect to the first two components  $\mu_I = m_I$  of  $\hat{\boldsymbol{\mu}}$  in equation C-2 one can write

$$\frac{\partial S}{\partial m_I} = \frac{\partial S}{\partial z_M} \frac{\partial z_M}{\partial m_I} + \frac{\partial S}{\partial z_3} \frac{\partial z_3}{\partial m_I}. \quad (\text{C-8})$$

Differentiation with respect to  $\mathbf{m}$  in equation C-8 is, by definition, performed for constant  $t^{\mathcal{Z}}$ . If  $\mathbf{m} = \mathbf{0}$  and  $t^{\mathcal{Z}} = 0$  we use equation C-5 to obtain

$$\frac{\partial S}{\partial m_I} = \frac{\partial S}{\partial z_M} \frac{\partial z_M}{\partial m_I}. \quad (\text{C-9})$$

- The situation  $k = 3$  in equation C-3 is described specifically by the equations

$$\frac{\partial t^z}{\partial z_M} \frac{\partial z_M}{\partial m_I} + \frac{\partial t^z}{\partial z_3} \frac{\partial z_3}{\partial m_I} = 0, \quad \frac{\partial t^z}{\partial z_M} \frac{\partial z_M}{\partial t^z} + \frac{\partial t^z}{\partial z_3} \frac{\partial z_3}{\partial t^z} = 1. \quad (\text{C-10})$$

Using equations C-5 and C-7 for  $\mathbf{m} = \mathbf{0}$  and  $t^z = 0$  then gives

$$\frac{\partial t^z}{\partial z_I} = 0, \quad \frac{\partial t^z}{\partial z_3} = \frac{1}{v_3^z}. \quad (\text{C-11})$$

### Surface-to-surface travelttime relation: first order

Differentiating equation C-1 with respect to  $\mathbf{z}$  yields

$$\frac{\partial t^z}{\partial z_M} = \frac{\partial t}{\partial z_M} - \frac{\partial \mathcal{T}}{\partial z_M}, \quad \frac{\partial t^z}{\partial \mathbf{z}} = \frac{\partial t}{\partial \mathbf{z}} - \frac{\partial \mathcal{T}}{\partial \mathbf{z}}. \quad (\text{C-12})$$

Using  $S = \mathcal{T}$  in equation C-9,

$$\frac{\partial \mathcal{T}}{\partial m_I} = \frac{\partial z_M}{\partial m_I} \frac{\partial \mathcal{T}}{\partial z_M}, \quad \frac{\partial \mathcal{T}}{\partial \mathbf{m}} = \mathbf{A}^T \frac{\partial \mathcal{T}}{\partial \mathbf{z}}, \quad (\text{C-13})$$

and the fact that  $\partial t^z / \partial \mathbf{z} = \mathbf{0}$  then shows that the vector form of equation C-12 can be restated as

$$\frac{\partial t}{\partial \mathbf{z}} = \mathbf{A}^{-T} \frac{\partial \mathcal{T}}{\partial \mathbf{m}}. \quad (\text{C-14})$$

Equation C-14 is a fundamental equation that can be used to relate the dip of the reflector to the gradient,  $\partial \mathcal{T} / \partial \mathbf{m}$ , of surface-to-surface travelttime. The vector  $\partial t / \partial \mathbf{z}$  contains the first two components of the slowness vector at the IIP. This slowness vector projection belongs to the local Cartesian  $(\mathbf{z}, z_3)$  coordinate system and is equivalently referred to as

$$\mathbf{p}^z = \frac{\partial t}{\partial \mathbf{z}}. \quad (\text{C-15})$$

### Surface-to-surface travelttime relation: second order

We differentiate the leftmost equation C-10 with respect to components  $m_J$  as follows,

$$\frac{\partial}{\partial m_J} \left( \frac{\partial t^z}{\partial z_M} \frac{\partial z_M}{\partial m_I} + \frac{\partial t^z}{\partial z_3} \frac{\partial z_3}{\partial m_I} \right) = 0. \quad (\text{C-16})$$

Working out the various terms yields

$$\frac{\partial z_M}{\partial m_I} \frac{\partial}{\partial m_J} \left( \frac{\partial t^z}{\partial z_M} \right) + \frac{\partial t^z}{\partial z_3} \frac{\partial^2 z_3}{\partial m_I \partial m_J} + \dots = 0, \quad (\text{C-17})$$

where the dots (...) signify terms that contain partial derivatives of the type  $\partial z_3 / \partial m_I$  or  $\partial t^z / \partial z_M$ . For  $\mathbf{m} = \mathbf{0}$  and  $t^z = 0$  all such terms are zero. We now apply equation C-1 in equation C-17 and insert the surface function  $z_3 = \Sigma^z(\mathbf{z})$ . Elaborating equation C-17 further utilizing the general differential operator in equation C-8, and finally requiring  $\mathbf{m} = \mathbf{0}$  and  $t^z = 0$ , we obtain

$$\frac{\partial^2 \mathcal{T}}{\partial m_I \partial m_J} = \frac{\partial z_M}{\partial m_I} \left( \frac{\partial^2 t}{\partial z_M \partial z_N} + \frac{\partial t^z}{\partial z_3} \frac{\partial^2 \Sigma^z}{\partial z_M \partial z_N} \right) \frac{\partial z_N}{\partial m_J}. \quad (\text{C-18})$$

In the above derivations, we have made use of the results

$$\frac{\partial z_M}{\partial m_I} \frac{\partial}{\partial m_J} \left( \frac{\partial t}{\partial z_M} \right) = \frac{\partial z_M}{\partial m_I} \frac{\partial^2 t}{\partial z_M \partial z_N} \frac{\partial z_N}{\partial m_J}, \quad (\text{C-19})$$

and

$$\frac{\partial z_M}{\partial m_I} \frac{\partial}{\partial m_J} \left( \frac{\partial \mathcal{T}}{\partial z_M} \right) = \frac{\partial z_M}{\partial m_I} \frac{\partial}{\partial z_M} \left( \frac{\partial \mathcal{T}}{\partial m_J} \right) = \frac{\partial^2 \mathcal{T}}{\partial m_I \partial m_J}, \quad (\text{C-20})$$

as well as the properties 7 of the reflector. Using the rightmost equation C-11 and also the definition of the reflector curvature matrix

$$D_{MN} = -\frac{\partial^2 \Sigma^Z}{\partial z_M \partial z_N}, \quad (\text{C-21})$$

also given by equation 7, our final result in component form appears as

$$\frac{\partial^2 \mathcal{T}}{\partial m_I \partial m_J} = \frac{\partial z_M}{\partial m_I} \left( \frac{\partial^2 t}{\partial z_M \partial z_N} - \frac{1}{v_3^Z} D_{MN} \right) \frac{\partial z_N}{\partial m_J}. \quad (\text{C-22})$$

The corresponding matrix form of equation C-22 is

$$\frac{\partial^2 \mathcal{T}}{\partial \mathbf{m} \partial \mathbf{m}^T} = \mathcal{A}^T \left( \frac{\partial^2 t}{\partial \mathbf{z} \partial \mathbf{z}^T} - \frac{1}{v_3^Z} \mathbf{D} \right) \mathcal{A}. \quad (\text{C-23})$$

Equation C-23 is a fundamental relation that relates the curvature matrix,  $\mathbf{D}$ , of the reflector to the second derivatives of the surface-to-surface traveltime,  $\partial^2 \mathcal{T} / \partial \mathbf{m} \partial \mathbf{m}^T$ .

The matrix  $\partial^2 t / \partial \mathbf{z} \partial \mathbf{z}^T$  contains second derivatives of the traveltime from the measurement surface taken along the tangent plane of the reflector. We can therefore compute this matrix as

$$\frac{\partial^2 t}{\partial \mathbf{z} \partial \mathbf{z}^T} = \mathcal{C}_0 \mathcal{A}^{-1}, \quad (\text{C-24})$$

where matrix  $\mathcal{C}_0$  is a special version of the submatrix  $\mathcal{C}$  contained within the surface-to-surface propagator matrix  $\mathcal{T}$ : matrix  $\mathcal{C}_0$  corresponds to evaluating matrix  $\mathcal{C}$  with zero reflector curvatures.